

On the origins of cathode hyperpolarization effects in electrolytic fluorine production from $\text{KF} \cdot 2\text{HF}$ melts

S. Y. QIAN, B. E. CONWAY

Chemistry Department, University of Ottawa, Ottawa, Ontario, K1N 6N5, Canada

Received 2 June 1993

The operation of electrolysis cells for fluorine production is accompanied by appreciable overvoltage effects not only at the anode but also appreciably at the steel cathode. This unexpected large overvoltage is referred to here as 'hyperpolarization' and sets in under certain conditions of current density and temperature which can lead to temporary failure of the cell operation. In a detailed study of hyperpolarization it has been found that its onset is very sensitive to the HF content in the $\text{KF} \cdot 2\text{HF}$ melt electrolyte, as demonstrated by a series of experiments in which the HF contents of the melt were systematically varied around the formal 1 : 2 $\text{KF} \cdot 2\text{HF}$ composition ratio. Experiments at a rotating cone mild-steel electrode, and one with a solidified melt, as well as studies of temperature effects, combined with the phase-diagram, provide evidence that the hyperpolarization arises on account of mass-transport limitation associated with HF consumption. The suddenness and 'irreversibility' of the onset of the hyperpolarization effect is directly related to HF starvation in the diffusion layer at high current-densities which, in turn, leads to a more significant effect, the onset of local solidification of the electrolyte in a thin film at the electrode interface. A computer simulation of the diffusion situation provides a firm basis for the interpretation of the origin and significance of the hyperpolarization effect.

1. Introduction

The electrolytic production of elemental fluorine, although not such an intensive and extensive commercial activity as the chlor-alkali process for chlorine (and NaOH) production, is nevertheless one of the significant industrial electrolytic processes. One of the reasons for this is that owing to the high electro-negativity of fluorine and its place at the 'bottom' of the electrochemical series, it can *only* be prepared by an electrolytic process with the exception of such exotic reactions as the decomposition of XeF_4 or XeF_6 .

The commercial production of elemental fluorine is directed mainly towards the preparation of UF_6 from uranium oxide ores for the purpose of obtaining pure uranium or isotopically-enriched uranium. Fluorine is also required in the preparation of some fluoro-carbons, perfluoro-organics and perfluoro-polymers such as Teflon.

The electrolytic production of fluorine is most conveniently achieved in commercial and laboratory practice by electrolysis of a $\text{KF} \cdot 2\text{HF}$ melt at about 85°C using a carbon anode and a suitable metal as cathode, for example mild-steel in the commercial operation. The cathodic process, conjugate to the anodic one of fluorine production, is evolution of molecular hydrogen by discharge from the HF/FHF^- system.

The operation of electrolysis cells for fluorine production is accompanied not only by a remarkably

large overvoltage at the anode [1] (a well known effect) but also, as we find here, by appreciable analogous overvoltage effects at the cathode. This large cathodic overvoltage can rise to 8 V or even higher (depending on the potentiostat or power supply) under certain operating conditions and lead to the failure of the cell operation. The development of the anomalous high cathodic overvoltage is referred to, here, as the 'hyperpolarization effect' but is different in origin from a corresponding behaviour at carbon anodes which has been referred to as the 'anode effect'. The latter has been the subject of considerable previous research [2, 3] including earlier contributions from this laboratory [1, 4].

Many studies have been carried out on the fluorine evolution reaction at carbon anodes, especially on the so-called 'anode effect' [2, 3], referred to above, but relatively little work, if any, has been done previously on *cathodic* hyperpolarization effects; only a brief mention of such effects is to be found in [5]. Determination of the origin of the latter effect at mild-steel cathodes in fluorine-production cells is important practically with regard to electric energy consumption and optimization of cell operation, and is also of substantial fundamental and theoretical interest.

In the present paper, the origin of the unusual cathode hyperpolarization has been studied in some detail and a new understanding of the phenomenon has been gained. The results show that mass-transport limitation due to HF consumption, leading

to reactant starvation at the electrode surface, arises resulting in local solidification of the electrolyte in a thin film at the electrode interface. This is found to be the principal reason which leads to hyperpolarization at the cathodes in fluorine-production cells and corresponding laboratory experiments on much smaller scales.

2. Experimental details

2.1. Cell

The experimental cell was fabricated by joining together two cylindrical plexiglass tubes in parallel vertical orientation with a small hole at the bottom between the two cylinders to provide a connection between the two compartments and also to keep apart the two gases, hydrogen and fluorine, which are evolved from the cathode and anode, respectively. The cylindrical shape was chosen to avoid turbulent flow of the melt when a rotating electrode used in some of the experiments was rotated at elevated rates.

The cell was mounted in an air-heated thermostat oven with the temperature being controlled at 85°C.

2.2. Rotating mild-steel cone cathode

A rotating electrode arrangement was found to be required (see below) to provide or enhance mass transfer of HF in the melt to the cathode working surface. Its conical form was necessary (as found in corresponding experiments at carbon anodes [1]) to facilitate gas bubble detachment which otherwise leads to anomalous and erratic polarization behaviour in the fluoride melt. This bubble effect is associated with the unusual surface tension and contact angle properties of interfaces with the KF·2HF melt as found in our related anode studies on fluorine evolution.

For the rotating electrode experiments a rotating mild-steel cone electrode was fabricated and tightly mounted in a Teflon cylinder having a 45° conical geometry. It was rotated in an analytical rotator (Pine Instrument Co., model ASR). The mild-steel material was of the same specification as that used in industrial cells. The cone electrodes were freshly polished in each series of experiments by means of 2400 silicon-carbide paper to maintain the electrode in a reproducible surface condition.

2.3. Counter electrode (anode)

The counter electrode was cut from a large porous carbon block of the kind used in commercial fluorine-production cells. It had dimensions 4 cm × 5 cm × 1 cm, giving about 50 cm² total apparent surface area exposed to the melt. A copper rod was threaded on to the carbon block counter electrode to provide an electric connection.

2.4. Reference electrodes

It was found that the Fe/FeF₂ reference electrode behaves very satisfactorily in the KF·2HF melt. Such electrodes were periodically checked against a Cu/CuF₂ electrode and the measured potentials were satisfactorily reproducible.

2.5. Electrolyte melt

The KF·2HF melt was made by slow stoichiometric addition of HF from a cylinder to KF·HF in a cooled vessel. The hydrogen fluoride (supplied by Matheson Co.) was 99.9% pure and the potassium hydrogen fluoride (obtained from Johnson Matthey) was of >99% purity. Together they were used to prepare the KF·2HF melt gravimetrically.

2.6. Electrochemical measurements

The steady-state polarization experiments were made using an Hokuto Denko HA-301 potentiostat, the resulting data being acquired by an on-line computer system, consisting of an HP microcomputer with a Keithley 195 Digital Multimeter and a Kepco Digital Programmer. The potential against time relations generated in some experiments were recorded digitally by a Nicolet 310 oscilloscope. The data was then transferred to an HP computer for processing and plotting.

3. Results and discussion

3.1. Hyperpolarization related to mass-transport limitations

At mild-steel cathodes in the KF·2HF melt, η increases linearly with $\log i$ with a slope, b , of about 0.11 V decade⁻¹ of change of current density, i , at 85°C, corresponding more or less to behaviour determined by the kinetics of discharge of the proton in HF at the electrode surface, as follows:

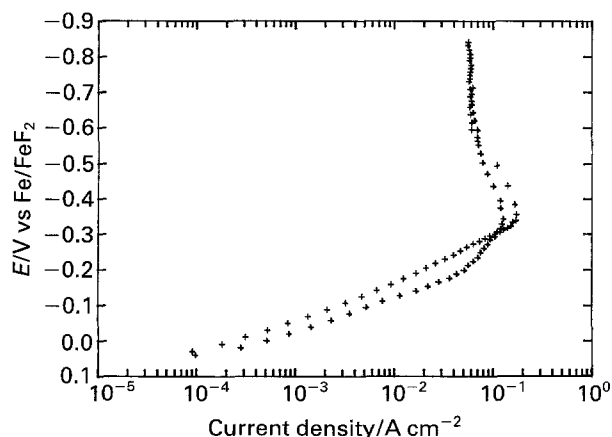
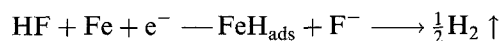


Fig. 1. Steady-state polarization behaviour of a mild steel electrode in KF·2HF melt at 85°C.

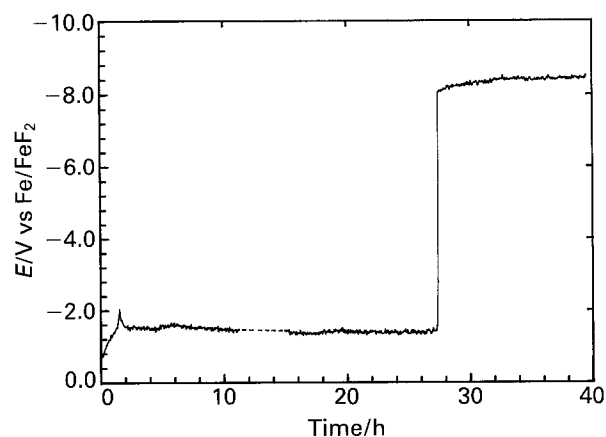


Fig. 2. Potential of a mild steel electrode polarized galvanostatically in $\text{KF} \cdot 2\text{HF}$ at 85°C .

However, as illustrated in Figs 1 and 2, when high current densities are attained, a state of hyperpolarization sets in with very high overvoltages being manifested after some time. Correspondingly, the electrolysis cell voltage substantially increases and leads, in practical cell operation, to excess power consumption, sometimes even leading to failure in cell operation.

A critical series of experiments showed that the hyperpolarization potential, V_{hp} , and the corresponding hyperpolarization limiting current, I_{lim} , (Figs 3 to 5) could be substantially modified by electrode rotation. The hyperpolarization voltage is substantially decreased with increase of electrode rotation rate; the effect is partly 'reversible', as the voltage increases again with decreasing rotation rate (Fig. 4). These results clearly indicate that there are substantial effects of mass-transport on the electrode polarization once the hyperpolarization sets in, as well as a much increased induction time for its onset when the electrode is rotated, depending on the actual rotation rate and the steady-state current that is passing.

3.2. The effect of HF content of the melt and the melt temperature on the hyperpolarization

The mass-transport limitation appears to be due to

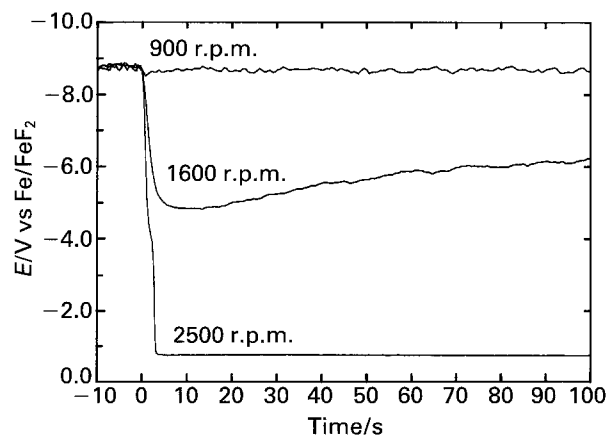


Fig. 3. Rotation effect on the 'hyperpolarization' potential at a mild-steel cone rotating electrode.

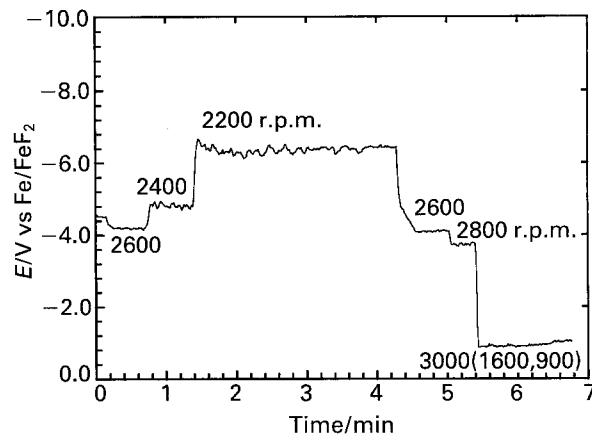


Fig. 4. Rotation effect on the hyperpolarization potential at a mild steel cone rotating electrode.

HF reactant starvation at the electrode surface on the inner side of the diffusion layer. This was quantitatively and unambiguously proved by a series of experiments in which the HF contents of melts were systematically varied around the formal 1:2 $\text{KF} \cdot 2\text{HF}$ composition ratio in relation to the determined phase equilibrium diagram (Fig. 6) for the system [5]. The results obtained showed quite clearly that the conditions (V_{hp} , I_{hp}) associated with the onset of hyperpolarization and the resulting hyperpolarization limiting current, $I_{\text{lim, hp}}$, at HF-consuming cathodes were sensitively dependent on the percentage HF in the melt (Fig. 7).

The hyperpolarization effect was also found to be appreciably dependent on the melt temperature: both the onset current, and the subsequent limiting current, increase appreciably already with only fairly small increases of temperature above the normal melting point of $\text{KF} \cdot 2\text{HF}$ as indicated by the data listed below in Table 1.

This situation arises owing to the proximity of the cell operating temperature to the melting point of $\text{KF} \cdot 2\text{HF}$ around a known phase-transition (see Fig. 6 and [5]) that is sensitively dependent on HF content in the KF -solvate melt. This suggests that the suddenness of the onset of the

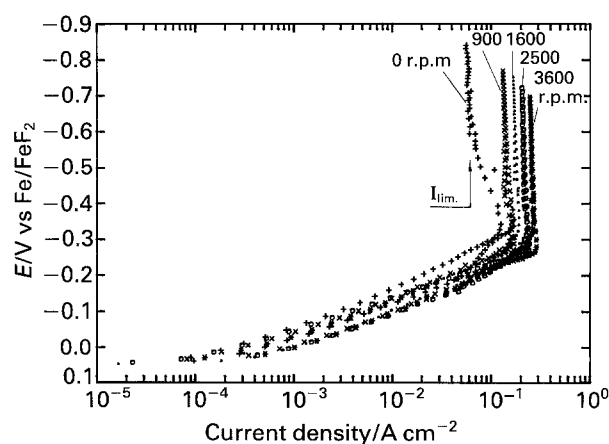


Fig. 5. Tafel plots for the hydrogen evolution reaction from a $\text{KF} \cdot 2\text{HF}$ melt at a mild steel cone electrode at different rotation speeds: (+ — +) 0; (× — ×) 900; (· — ·) 1600; (○ — ○) 2500; and (* — *) 3600 r.p.m. Temperature: 85°C .

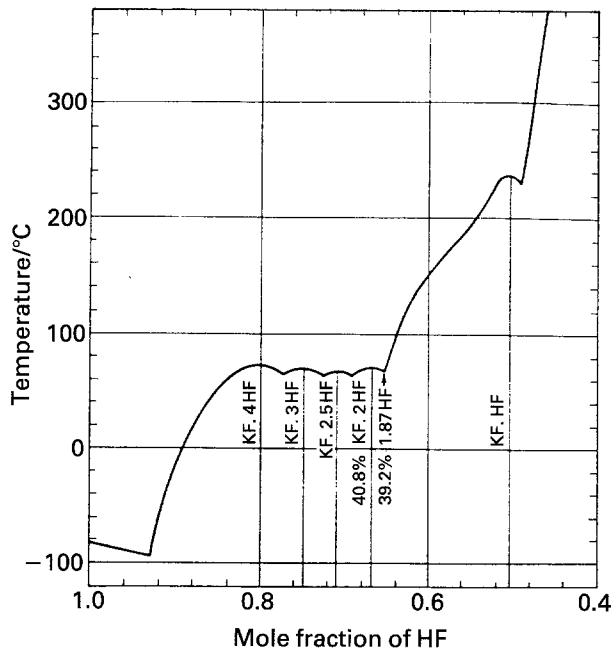


Fig. 6. Melting point/composition diagram for the potassium fluoride/hydrogen fluoride system.

effect caused at high polarization current-densities is due to a more significant effect, *local solidification*, of the electrolyte in a thin film at the electrode interface with consequent development locally of a high interfacial resistance at the mild-steel surface when a critical level of HF starvation becomes established.

The HF content of the melt determines presumably the steady-state thickness of a solid 'KF-HF' film that can be formed; the formation of that film also depends on the temperature and whatever forced convection conditions obtain.

It was found that even below the melting point of KF·2HF, current can *still* be passed and the polarization relation for the electrode kinetic behaviour in solid KF·2HF just *below* its melting point is shown by the steep line on the left-hand side of the main polarization curve of Fig. 8. Its slope is similar to that of the polarization curve (Fig. 8) for descending potentials just after attainment of the limiting

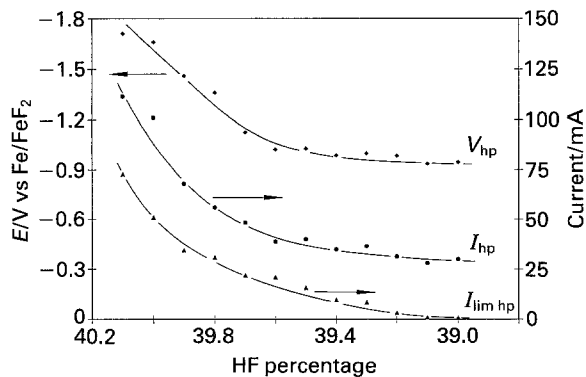


Fig. 7. Effect of HF percentage in the 'KF·2HF' melt on the potential, V_{hp} (◆) and the current, I_{hp} (●) for onset of hyperpolarization and on the hyperpolarization limiting current, $I_{lim\ hp}$ (▲). Temperature: 85°C.

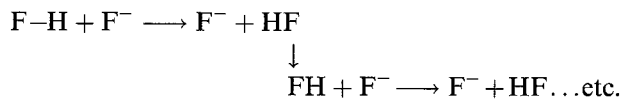
Table 1. The relation between the hyperpolarization current conditions and temperature

Current	Temperature		
	85°C	90°C	98°C
I_{hp}/mA	31	40	63
$i_{hp}^*/\text{mA cm}^{-2}$	110	143	225
I_{lim}/mA	0.22-0.34	8	24
$i_{lim}^*/\text{mA cm}^{-2}$	0.79-1.2	29	86

* Electrode surface area 0.28, cm²

current. This supports the interpretation of the hyperpolarization effect as being due to generation of a thin, resistive solid film at the electrode interface due to HF starvation, with consequent increase of the melting point of the electrolyte just in the diffusion boundary layer.

The significant currents that still pass in the *solid state* must be due to the possibility of proton conduction in the KF·2HF solid. The situation is evidently similar to that in the solid hydrate, HClO₄·5.5H₂O, studied by Stimming [6] who showed that electrochemistry could be performed in this medium even down to some 80°C below its melting point. We have observed similar behaviour in the hydrogen-bonded, solid hydronium salt H₃O⁺·CF₃SO₃⁻. In the KF-HF case the conductivity (as with HClO₄ hydrate) can arise from proton hopping, like the proton conductance mechanism in acid or alkaline aqueous solutions [7, 8], thus



Such a process can continue in the solid state as is known, for example, for proton transport in ice [9].

3.3. Computer simulation of the onset of the hyperpolarization

It has been proposed above that the hyperpolarization behaviour arises on account of mass-transport

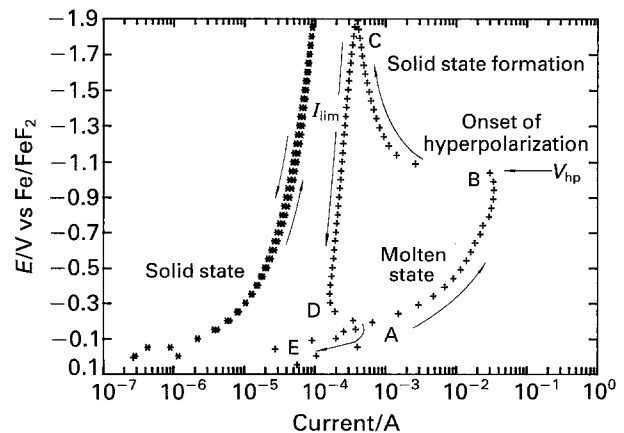


Fig. 8. The polarization behaviour at a mild-steel electrode in molten (+) against solid (*) KF·2HF near its melting point.

limitation associated with HF consumption at the electrode and resulting melting point change of the electrolyte in the vicinity (diffusion boundary layer) of the electrode interface. This interpretation of the polarization behaviour was tested by means of a computer simulation calculation of the supposed diffusion-controlled depletion of HF, as follows.

By solving the equation for nonstationary convective diffusion, the diffusion current, I , can be obtained for an electrode of area, A , as

$$I = \frac{nFA}{\nu} (C_{\text{HF}}^0 - C_{\text{HF}}^s) \left(\frac{D_{\text{HF}}}{\pi t} \right)^{1/2} \quad (1)$$

where ν is the kinematic viscosity of the melt. In the potassium fluoride/hydrogen fluoride system, the ν would change with the polarization time, t , because of HF consumption at the electrode surface and the melting point of the melt increases due to the 'HF starvation'. The kinematic viscosity would also tend to increase with polarization time after hyperpolarization has set in. It is obviously difficult to know how the kinematic viscosity of the melt exactly changes with polarization time; we therefore assume here it has the following relation:

$$\nu = \nu^0 \cdot t^x \quad (x > 0) \quad (2)$$

where the ν^0 is the initial kinematic viscosity of the melt. The value of x will depend on the HF concentration in the melt; it determines, practically, the rate of change of kinematic viscosity, ν , with t during the experiment. Its value is selected empirically (see below).

The polarization V against $\log I$ behaviour is experimentally measured by application of a series of very small steps of increased potential applied to the electrode, and the relation between potential and time is represented by $V = st$ where s is a resulting average potential scan rate derived from the calculation of the periodic potential-step increase in relation to its duration.

To fit the experimental V against $\log I$ measurements in that way, the potential, V , against time, t , relation also has to meet following conditions:

$$\begin{cases} V = V_{\text{init}} - st \\ V = -1.9 + (st - V_{\text{init}} - 1.9) \end{cases} \quad \text{when } \begin{cases} 0 < t < (1.9 + V_{\text{init}})/s \\ \text{or } t > (1.9 + V_{\text{init}})/s \end{cases} \quad (3)$$

where V_{init} is the initial potential at which diffusion control starts to dominate the reaction kinetic behaviour at the electrode and the -1.9V is the upper potential of the measurement programme at which the V against $\log I$ is of measurements change direction.

On substituting the expressions for ν and t into Equation 1, the relation of potential, V , to current,

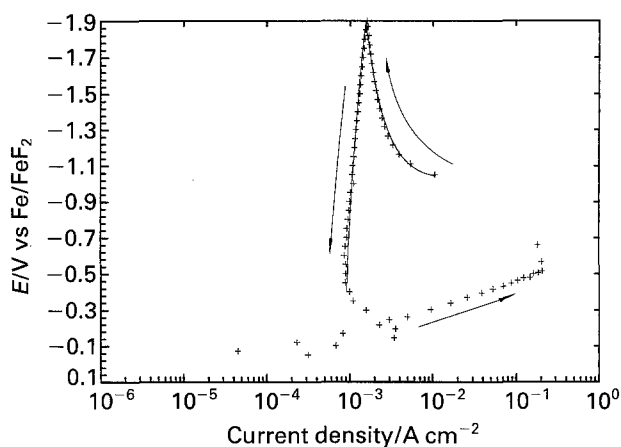


Fig. 9. The polarization behaviour at the mild-steel electrode in a melt with partially consumed HF (+ + +) and simulated results by using the modified nonstationary diffusion equation (—).

I , is obtained as

$$\begin{cases} I = \frac{nFA(C_{\text{HF}}^0 - C_{\text{HF}}^s)}{\nu^0 [(V_{\text{init}} - V)/s]^x} \times \left(\frac{D_{\text{HF}}}{\pi [(V_{\text{init}} - V)/s]} \right)^{1/2} & \text{when } V_{\text{init}} > V > -1.9 \\ I = \frac{nFA(C_{\text{HF}}^0 - C_{\text{HF}}^s)}{\nu^0 [(V + 3.8 + V_{\text{init}})/s]^x} \times \left(\frac{D_{\text{HF}}}{\pi [(V + 3.8 + V_{\text{init}})/s]} \right)^{1/2} & \text{when } V < -1.9 \end{cases} \quad (4)$$

Figure 9 shows the computer simulation results, using Equation 4 taking $(D_{\text{HF}})^{1/2} C_{\text{HF}}^0 / L^0 = 2.73 \times 10^{-10} \text{ mol cm}^{-4} \text{ s}^{1/2}$, $F = 96500 \text{ C}$ with $C_{\text{HF}}^0 = 38 \times 10^{-3} \text{ mol cm}^{-3}$, $V_{\text{init}} = -1.02 \text{ V}$ and adjusting the value of the exponent x to 0.7. It is seen that the curve (solid line) for the simulation calculations reproduces excellently almost the whole form of the experimental curve (+ points) both in the directions of ascending and descending potential changes.

The above test provides a firm basis for the interpretation of the origin and significance of the hyperpolarization effect as arising from diffusion-controlled depletion of HF reactant with associated local solidification of the melt.

The whole polarization behaviour can be accounted for in terms of the above model and calculations of the hyperpolarization effect, refer to Fig. 8, as follows.

- (i) At low current-densities, the HF content has no appreciable effect on the polarization behaviour; HF can be sufficiently rapidly transported by diffusion to the electrode interphase to meet the consumption rate corresponding to the low current densities.
- (ii) At a critical current-density (the critical value for onset of hyperpolarization), no further increase of i with V arises.
- (iii) Beyond this point (ii) i decreases with time and potential towards a *limiting current density*, substantially less than the earlier i for the onset of hyperpolarization.
- (iv) Upon decrease of overpotential a more or less constant limiting i is maintained until, at high enough V .

(v) Some reactivation of the hydrogen evolution process takes place due, we believe to the remelting of the film with return to normal HF supply conditions. Then, at further, higher V 's and correspondingly diminished i 's.

(vi) Normal Tafel $\log i$ against V behaviour is again observed and the behaviour returns to that in (i).

4. Conclusions

(i) The hyperpolarization behaviour observed in cathodic hydrogen evolution from $\text{KF} \cdot 2\text{HF}$ melts arises on account of mass-transport limitation associated with HF consumption. Rotation of the mild-steel cone electrode has a strong effect on the rate of the hydrogen evolution reaction once the hyperpolarization has set in.

(ii) The suddenness and 'irreversibility' of the onset of the hyperpolarization effect is directly related to the HF starvation in the diffusion-layer at high current densities which, in turn, leads to a more significant effect, the local solidification of the electrolyte in a thin film at the electrode interface with consequent development locally of a high ohmic resistance at the mild steel surface.

(iii) The hyperpolarization effect is appreciably dependent also on the melt temperature. With increase of temperature, both the onset currents and the subsequent limiting currents increase appreciably. The temperature effect is clearly related to the phase diagram for the solidus/liquidus boundary, which determines the melting points of various compositions of the melt around the ' $\text{KF} \cdot 2\text{HF}$ ' composition.

(iv) The results suggest that some forced circulation of the melt in industrial cells, additional to that caused by adventitious bubble stirring and magneto-

hydrodynamica effects, may be advantageous in preventing periodic onset of hyperpolarization in operating fluorine-production cells.

Acknowledgements

Grateful acknowledgement is made to the Natural Sciences and Engineering Research Council of Canada for support of this work on a joint project with 'Cameco - A Canadian Mining and Energy Corporation'. Special thanks are due to Drs D. G. Garratt, T. Zawidzki and M. Watson for many stimulating discussions during this research project and to Dr Garratt for his support during its execution and also to Cameco Corporation for their component of the financial support of this project which has continued beyond the completion date of the initial NSERC cooperative research and development agreement.

References

- [1] L. Bai and B. E. Conway, *J. Appl. Electrochem.* **18** (1988) 839-848.
- [2] N. Watanabe, M. Ishii and S. Yoshizawa, *J. Electrochem. Soc. Jpn.* **29** (1961) E 180; see also N. Watanabe, *Proc. Electrochem. Soc., Electrochemistry of Carbon* (1984) p. 536.
- [3] D. Devilliers, F. Lantelme and M. Chemla, *Electrochim. Acta* **31** (1986) 1235.
- [4] L. Bai and B. E. Conway, *J. Appl. Electrochem.* **20** (1990) 916-931.
- [5] A. J. Rudge, in 'Industrial Electrochemical Processes' (edited by A. T. Kuhn), Elsevier, Amsterdam (1971) Chapter 1.
- [6] U. Frese and U. Stimming, *J. Electroanal. Chem.* **198** (1986) 409.
- [7] J. D. Bernal and R. H. Fowler, *J. Chem. Phys.* **1** (1933) 515.
- [8] B. E. Conway, J. O'M. Bockris and H. Linton, *ibid.* **24** (1956) 834.
- [9] M. Eigen and L. de Macyer, *Z. Elektrochem.* **60** (1956) 1037.